Published in final edited form as:

Neurobiol Dis. 2018 August ; 116: 120–130. doi:10.1016/j.nbd.2018.05.001.

Regulation of seizure-induced MeCP2 Ser421 phosphorylation in the developing brain

Evan C. Rosenberg[b,c,1], **Jocelyn J. Lippman-Bell**[a,b,d,1], **Marcus Handy**[a], **Samantha S. Soldan**[a], **Sanjay Rakhade**[b], **Cristina Hilario-Gomez**[b], **Kaitlyn Folweiler**[a], **Leah Jacobs**[a], **Frances E. Jensen**[a,b,*]

[a]Perelman School of Medicine, University of Pennsylvania, Department of Neurology, Philadelphia, PA 19104, United States

[b]Boston Children's Hospital, Department of Neurology, Boston, MA 02115, United States

[c]New York University Langone Medical Center, New York, NY 10016, United States

[d]Philadelphia College of Osteopathic Medicine, Department of Biomedical Sciences, Philadelphia, PA 19131, United States

Abstract

Neonatal seizures disrupt normal synaptic maturation and often lead to later-life epilepsy and cognitive deficits. During early life, the brain exhibits heightened synaptic plasticity, in part due to a developmental over-abundance of $Ca_V1.2$ L-type voltage gated calcium (Ca^{2+}) channels (LT-VGCCs) and Ca^{2+}-permeable AMPARs (CP-AMPARs) lacking GluA2 subunits. We hypothesized that early-life seizures overactivate these channels, in turn dysregulating Ca^{2+}-dependent signaling pathways including that of methyl CPG binding protein 2 (MeCP2), a transcription factor implicated in the autism spectrum disorder (ASD) Rett Syndrome. Here, we show that *in vivo* hypoxia-induced seizures (HS) in postnatal day (P)10 rats acutely induced phosphorylation of the neuronal-specific target of activity-dependent MeCP2 phosphorylation, S421, as well as its upstream activator CaMKII T286. We next identified mechanisms by which activity-dependent Ca^{2+} influx induced MeCP2 phosphorylation using *in vitro* cortical and hippocampal neuronal cultures at embryonic day (E)18 + 10 days *in vitro* (DIV). In contrast to the prevalent role of NMDARs in the adult brain, we found that both CP-AMPARs and LT-VGCCs mediated MeCP2 S421 and CaMKII T286 phosphorylation induced by kainic acid (KA) or high potassium chloride (KCl) stimulation. Furthermore, *in vivo* post-seizure treatment with the broad-spectrum AMPAR antagonist NBQX, the CP-AMPAR blocker IEM-1460, or the LT-VGCC antagonist nimodipine blocked seizure-induced MeCP2 phosphorylation. Collectively, these results demonstrate that early-life seizures dysregulate critical activity-dependent developmental signaling pathways, in part *via* CP-AMPAR and LT-VGCC activation, providing novel age-specific therapeutic targets for convergent pathways underlying epilepsy and ASDs.

*Corresponding author at: Department of Neurology, Perelman School of Medicine, University of Pennsylvania, 3400 Spruce Street, Philadelphia, PA 19104-4283, United States. frances.jensen@uphs.upenn.edu (F.E. Jensen).

[1]ECR and JJL contributed equally to this work. Current address for CHG is Istituto Italiano di Tecnologia, 16163 Genova, Italy.

Appendix A. Supplementary data

Supplementary data to this article can be found online at https://doi.org/10.1016/j.nbd.2018.05.001.

Keywords

MeCP2; Seizure; Rett Syndrome; Autism spectrum disorder; AMPARs; LT-VGCCs

1. Introduction

The neonatal brain exists in a heightened state of excitation, primed for activity-dependent synaptic plasticity, formation, and refinement (Rakhade and Jensen, 2009). This hyperexcitability, although ideal for learning and memory, renders the brain vulnerable to seizures (Ben Ari and Holmes, 2006; Jensen et al., 1992; Rakhade and Jensen, 2009; Wirrell et al., 2011). Early-life seizures can alter development and plasticity of neuronal circuitry (Hernan et al., 2013; Isaeva et al., 2013; Swann, 2004; Zhou et al., 2011), which may in turn lead to cognitive impairments and autistic-like behavior (Brooks-Kayal, 2010; Lippman-Bell et al., 2013; Lucas et al., 2011; Lugo et al., 2014). Notably, many genetic autism spectrum disorders (ASDs) exhibit early-onset seizures (Berg et al., 2011; Tuchman, 2013), indicating a convergence of cellular and molecular mechanisms in ASDs and seizures. Activity-dependent synaptogenesis and downstream signaling may be an important area for therapeutic target development in treating these disorders.

Hypoxic encephalopathy, the leading clinical cause of neonatal seizures (Glass and Ferriero, 2007; Minchom et al., 1987), can be refractory to conventional antiepileptic drugs and can result in later-life epilepsy and cognitive and behavioral deficits (Brooks-Kayal, 2011; Jensen, 2009; Rakhade and Jensen, 2009; Tekgul et al., 2006). Consistently, studies using our established model of hypoxic seizures (HS) have demonstrated that only 15-minute hypoxia during the early-life critical period can produce profound, lasting deficits in naïve, wild type animals, including the development of later-life autistic-like social behavioral deficits (Lippman-Bell et al., 2013; Talos et al., 2012), subsequent spontaneous seizures (Rakhade et al., 2011), and increased susceptibility to “second-hit” kainic acid-induced seizures (Koh et al., 2004). Similarly, prior studies using other models of early-life seizures demonstrated severe impairments in learning, cognition, and sociability in later-life (Castelhano et al., 2013; Chang et al., 2003; Dube et al., 2009; Holmes et al., 1998; Huang et al., 2002; Sayin et al., 2004); although notably, our paradigm of HS does not produce confounding effects of cell death seen in other models (Lippman-Bell et al., 2016; Rakhade et al., 2011; Sanchez et al., 2001). Interestingly, our findings have demonstrated that HS preserve the brain in a hyperexcitable state, with strengthened excitatory synaptic strength (Rakhade et al., 2008), reduced silent synapses (Zhou et al., 2011), increased Ca^{2+} influx (Lippman-Bell et al., 2016), potentiated Ca^{2+} -dependent kinase signaling (Lippman-Bell et al., 2016; Rakhade et al., 2008; Sanchez et al., 2001; Talos et al., 2012) and glutamate receptor phosphorylation (Rakhade et al., 2008). Strikingly, each of these post-HS consequences are prevented by post-seizure blockade of the AMPA receptor (AMPAR) subtype of excitatory glutamate receptors, but not NMDA receptor antagonists (Jensen et al., 1995; Jensen and Wang, 1996).

In contrast to the adult, in which NMDARs primarily mediate activity-dependent, synaptically-driven Ca^{2+} signaling (Zhou et al., 2006), the immature brain contains Ca^{2+} -

permeable, GluA2-lacking AMPARs (Talos et al., 2006a,b), which significantly contribute to developmentally relevant intracellular signaling (Cull-Candy et al., 2006; Henley and Wilkinson, 2016; Rakhade and Jensen, 2009). Furthermore, $Ca_V1.2$ LT-VGCC expression is also developmentally upregulated in this same period of the second postnatal week (Kramer et al., 2012; Morton et al., 2013; Schlick et al., 2010). Given the protective effects of AMPAR blockers in our early-life *in vivo* seizure model compared with other glutamate receptor antagonists (Jensen et al., 1995; Jensen and Wang, 1996), we asked whether over-activation of CP-AMPARs and LT-VGCCs in early-life seizures might disrupt signaling pathways relevant to neurodevelopment.

Specifically, we examined whether AMPARs and LT-VGCCs regulate activity-dependent phosphorylation of the transcriptional regulator methyl CpG binding protein 2 (MeCP2) as one potential pathway linking early-life seizures to synaptic deficits. MeCP2 plays important roles in synaptic plasticity, dendritic development, and neuronal maturation during early postnatal life (Cohen et al., 2011; Feldman et al., 2016; Jiang et al., 2013; Kishi and Macklis, 2010; Luikenhuis et al., 2004; Mullaney et al., 2004; Shahbazian et al., 2002b; Zhou et al., 2006), and mutations in MeCP2 lead to the ASD Rett Syndrome (Amir et al., 1999). Furthermore, animal models of both neonatal hypoxic seizures (Lippman-Bell et al., 2013; Rakhade et al., 2011; Talos et al., 2012) and MeCP2 KO mice (Neul et al., 2010; Zhang et al., 2014) develop later-life ASD-like behavior, cognitive deficits, and increased seizure susceptibility, prompting the question of whether early-life seizures perturb MeCP2 function to initiate a process leading to synaptic and cognitive dysfunction.

Of the multiple phosphorylation sites that regulate MeCP2 function (Bellini et al., 2014), the neuronal-specific (Zhou et al., 2006) S421 site is highly regulated by activity, such as Schaffer collateral stimulation (Munoz et al., 2016), psychostimulant-induced plasticity (Deng et al., 2010, 2014), postsynaptic Ca^{2+} influx, and CaMKII T286 phosphorylation (Zhou et al., 2006). In older animals, NMDARs are the primary mediator of synaptically driven MeCP2 S421 phosphorylation (Zhou et al., 2006); however, we hypothesized that elevated expression of CP-AMPARs and LT-VGCCs early in development may provide an additional route of Ca^{2+} entry into neurons (Morton et al., 2013; Rakhade and Jensen, 2009; Sanchez et al., 2001).

Here we present evidence that *in vivo* neonatal seizures and *in vitro* neuronal depolarization induce phosphorylation of MeCP2 and its upstream activator CaMKII. Further, we demonstrate that two developmentally-regulated targets, CP-AMPARs and LT-VGCCs, mediate seizure-induced MeCP2 S421 phosphorylation. Our results highlight potential age-specific treatment options following early-life seizures, and provide evidence for at least one pathway of overlap between early-life seizures and ASDs.

2. Materials and methods

2.1. Animals

All studies were performed on male Long–Evans rats (Charles River Laboratories, Wilmington, MA, 10 pups/litter). Animals were housed in a temperature-controlled animal care facility with a 12-hour light/dark cycle and monitored regularly. All procedures were

approved by the Institutional Animal Care and Use Committees at Boston Children's Hospital and University of Pennsylvania, and in accordance with the NIH Guide for the Care and Use of Laboratory Animals. All efforts were made to minimize animal suffering and numbers.

2.2. Hypoxia-induced seizures

Hypoxic seizures (HS) were induced in postnatal day (P)10 pups as described (Sanchez et al., 2001). Pups were placed in an airtight chamber with a heating pad and exposed to graded 100% nitrogen infusion for 15 min, reducing O_2 concentrations to 7% O_2 for 8 min, 5% O_2 for 6 min, and 4% O_2 for 1 min. Age- and weight-matched littermate control pups were removed from their dam and placed on a heating pad, but not exposed to hypoxia. Seizures were defined as automatisms followed by head and limb movements and myoclonic jerks. To reduce variability, only animals with > 5 seizures were included in the study. Rats were sacrificed at 0.5, 1, 3, 6, and 24 h following HS (along with normoxic littermate controls). For drug treatment studies, P10 rats were given an intraperitoneal injection of either 20 mg/kg NBQX (Sigma, saline vehicle), 20 mg/kg IEM-1460 (Tocris, saline vehicle), 5 or 10 mg/kg nimodipine (Sigma, 10% DMSO/50% polyethylene glycol/40% dH_2O vehicle), or corresponding vehicle, within 30 min post-HS.

2.3. Dissociated cell culture preparation

Dissociated cortical and hippocampal neuronal cultures were prepared from Long-Evans rats at E17/18 as previously described (Xia et al., 1996). Dishes were coated with 50 μg/ml Poly-D-Lysine and 20 μg/ml Laminin 24 h before plating. Neurons were maintained in a Neurobasal solution (Gibco/Invitrogen), supplemented with B27 (Invitrogen), 100 U/ml penicillin/streptomycin (Invitrogen), and 2 mM L-glutamine (Sigma). Cells were plated at 1–1.5 × 10^6 cells/well in 6 well plates for immunoblotting, and 1 × 10^5 cells/well in 24 well plates for imaging.

2.4. Immunoblots

For *in vivo* studies, cortical tissue was dissected at designated time points following HS, combined from 3 rats per sample, rapidly frozen in ethanol, and stored at −80 °C. Nuclear lysates were isolated as previously described (Wang et al., 2012) using 1 protease and phosphatase inhibitor cocktail tablet (Thermo) per 10 ml buffer.

For *in vitro* studies, cells were treated for 2 h with 1 μM tetrodotoxin (TTX, Tocris), 100 μM D-APV (Tocris), 50 μM NBQX (Tocris), 150 μM NASPM (Sigma), 5 μM nimodipine (Tocris), 5 μM KN-92 (Calbiochem), 5 μM KN-93 (Calbiochem), and/or 1 mM EGTA (Sigma). Neurons were then stimulated for 1 h with 100 μM KA (Tocris) or 55 μM KCl (Sigma). Following stimulation, cells were harvested in 1 × Laemmli's Sample Buffer, prepared as whole-cell lysates, and run on gels as previously described (Talos et al., 2012).

For both *in vitro* and *in vivo* samples, total protein concentrations were measured using a Bradford protein assay (Bio-Rad). Samples were diluted for equal amounts of protein in each lane. Proteins were electrophoresed onto Bis-Tris gels, then transferred to polyvinylidene difluoride membranes (Bio-Rad). Immunoblots were incubated with primary

antibodies at 4 °C overnight (described below). After incubating with horseradish peroxidase-conjugated anti-rabbit IgG secondary antibodies (1:5000, Pierce), protein bands were visualized with enhanced chemiluminescence (Super-West Femto Maximum Sensitivity Substrate reagent, Thermo Fisher Scientific) and measured with the Image Reader LAS-3000 system and Image Gauge v3.0 software (Fujifilm).

For analysis, we performed separate blots for phospho- and total MeCP2 proteins with identical samples, due to the low sensitivity of the antibody following multiple strippings. Blots were incubated with the following primary antibodies: phospho-MeCP2 (S421) (1:1000) and total-MeCP2 (1:1000, kind gifts from Dr. Michael Greenberg, Harvard Medical School), phospho-CaMKII (T286) (1:250, Cell Signaling), and pan-CaMKII (1:250, Cell Signaling). To control for loading, blots were stripped and imaged for β-actin (1:5000, Sigma) for *in vitro* whole cell and Lamin A/C (1:1000, Cell Signaling) or Sin3a (1:100, Millipore) for *in vivo* nuclear samples. Following loading control normalization, ratios of phospho-/total MeCP2 (or CaMKII) ratios were measured, and normalized to either vehicle treated condition *(in vitro*) or age-matched normoxic controls *(in vivo*). For total MeCP2 quantification, we considered both bands for analysis - the phosphorylated (upper) and de-phosphorylated (lower) forms, as described (Zhou et al., 2006).

2.5. Calcium imaging analysis and controls

Ratiometric Ca^{2+} imaging was performed on cultures pretreated for 2h with 1 μM tetrodotoxin (TTX, Tocris), loaded with 15–20 μM Fura-2 AM (Invitrogen) and 0.1% pluronic F-127 (Invitrogen) for 30 min, then washed for 30 min. (All solutions hereafter were made in warmed, oxygenated ACSF containing 1 μM TTX). After 10 min bath application of 100 μM D-APV (Tocris), cells were stimulated using fast (< 2 min) treatment of 30 μM kainic acid (KA). After washout, cells were treated for 10 min with D-APV plus 50 μM NBQX (Tocris) or 150 μM 1-Napthylacetyl Spermine (NASPM, Sigma), then stimulated with KA again. Images were captured every 5 s on a Nikon Eclipse TE-2000S inverted microscope PlanFluor 20×/0.50 objective (∞/0/17, WD2.1). Changes in Ca^{2+} influx were assessed by change in 340/380 nm excitation ratio from baseline in individual somas (using regions of interests) in NisElements software. In all cells with a greater than background response to KA, change in peak Ca^{2+} response to KA before and after NASPM or NBQX treatment was analyzed *via* by paired *t*-test. Intracluster correlation was performed as described in detail previously (Aarts et al., 2014) to determine the effective n's. Two sets of control experiments were run alongside the primary experiments, in both cortical and hippocampal cultures: 1) Double stimulation with KA to ensure that the second stimulation does not degrade the calcium signal, and 2) Stimulation with KA with no prior antagonist treatment followed by APV application and an additional KA stimulation, to assess a baseline level for NMDAR presence in the cultures.

2.6. Immunocytochemistry

Surface receptor staining in live cultured neurons was performed as described (Hughes et al., 2010). Cells were incubated in culture media with an antibody directed against the extracellular domain of GluA2 (1:500, Millipore) for 1 h at 37 °C, then washed with conditioned media from adjacent wells and incubated with AlexaFluor 555 secondary

antibody (Invitrogen) for 1 h at 37 °C. Cells were then washed and fixed in 4% paraformaldehyde, 4% sucrose in PBS for 10 min, washed, per-meabilized with cold 0.2% Triton X-100 for 5 min, and blocked in 10% normal goat serum/0.1% Triton X for 1 h at room temperature. Cells were then labeled with antibodies against GluA1 (1:500, Abcam) and MAP2 (1:500, Millipore) to label dendrites. Antibodies were visualized with the appropriate AlexaFluor secondaries. Cells were imaged using a Zeiss LSM710 confocal microscope with an oil-immersion 63 × 1.7 NA objective. Colocalization analyses were performed *via* Image J and Icy (http://icy.bioimageanalysis.org) software. Regions of interest were traced around apical dendrites within the MAP2 channel, and % puncta colocalization between GluA1 and GluA2 puncta within a 0.5 μm radius was determined *via* the Icy Spot Detector Plugin. All analyses were performed blinded to developmental age.

2.7. Statistical analysis

Group data were expressed as mean ± SEM, with *n* representing the number of cortical samples (*in vivo*) or coverslips (*in vitro*), unless stated otherwise. Ca^2 + imaging experiments were analyzed *via* paired 2-way Student's *t*-test or 1-way ANOVA. For multiple comparisons across > 2 conditions, one-way ANOVA followed by *post hoc* Tukey's or Bonferroni multiple comparison tests were used. For the *in vivo* post-seizure time-course experiments, two tailed *t*-tests corrected for multiple comparisons with the Holm-Sidak method were used. Statistical significance was defined as $p < 0.05$.

3. Results

3.1. In vivo hypoxic seizures (HS) in P10 rats induce phosphorylation of MeCP2 S421 and CaMKII T286

Hypoxic seizures (HS) in neonatal rats (P10) induce rapid post-translational modifications and synaptic accumulation of AMPARs (Rakhade et al., 2008, 2012) and dysregulate several intracellular signaling cascades (Talos et al., 2012). We hypothesized that HS at P10, an age with high levels of CP-AMPARs and $Ca_V1.2$ channels (Morton et al., 2013; Talos et al., 2006a), would increase phosphorylation of MeCP2 and its upstream activator CaMKII. Indeed, cortical tissue removed post-HS showed a significant increase in MeCP2 S421 phosphorylation at 3h post-HS (Suppl. Fig. 1, Fig. 1A: 148 ± 11% *vs*. normoxic controls, $p = 0.003$), and elevated CaMKII T286 phosphorylation at 1 h post-HS (Fig. 1B: 184 ± 20% $p = 0.009$). These findings indicate that *in vivo* early-life seizures induce transient activity-dependent regulation of CaMKII and MeCP2.

3.2. Identification of functional CP-AMPARs at E18 + 10DIV

To determine whether CP-AMPARs facilitate HS-mediated MeCP2 and CaMKII phosphorylation in early life, we next examined their role in activity-dependent signaling in developing cortical and hippocampal primary neurons *in vitro*. We hypothesized that GluA2-lacking CP-AMPARs in young (E18 + 10DIV) neuronal cultures (Yin et al., 1999) and early postnatal rodent and human brains *in vivo* (Talos et al., 2006a,b) would provide an added source of synaptically driven Ca^{2+} to supplement signaling through NMDARs reported previously in more mature neurons (Zhou et al., 2006). To confirm the presence of CP-AMPARs, we measured neuronal Ca^{2+} influx *via* Fura-2 Ca^{2+} imaging in E18 + 10DIV

cultured cortical and hippocampal neurons stimulated by kainic acid (KA, 30 μM). KA-induced Ca^{2+} influx was reduced by the NMDAR antagonist D-APV (100 μM), suggesting that NMDA receptors contribute to about 25% of Ca^{2+} influx (Fig. 2A–B, normalized mean peak ratio in cortex (C): 100 ± 2% KA only *vs.* 74 ± 3% KA + APV, $p < 0.0001$; and hippocampus (H): 100 ± 3% KA only *vs.* 73 ± 3% KA + APV, $p < 0.0001$). The remaining NMDAR-insensitive Ca^{2+} influx (Fig. 2A, B, KA + APV C: 100 ± 3%, H: 100 ± 3%) was further decreased by both the AMPAR antagonist NBQX (50 μM) (C: 3 ± 2%, H: 31 ± 2%, *vs.* KA + APV condition, $p < 0.0001$) and 150 μM NASPM, a specific blocker of Ca^{2+} permeable, GluA2-deficient AM-PARs (C: 79 ± 3%, H: 84 ± 3%, $p < 0.0001$). Control neurons responded equally to dual KA stimulation (Suppl. Fig. 2A), excluding the possibility that reduced Ca^{2+} influx was due to repeated KA stimulation. Together, these findings confirm that CP-AMPARs facilitate part of the non-NMDAR-mediated Ca^{2+} influx at E18 + 10DIV.

Given the critical role of the GluA2 subunit in regulating Ca^{2+} permeability, we next used immunocytochemistry to measure the percentage of GluA1 subunits colocalized with GluA2. Consistent with prior reports (Kumar et al., 2002; Pickard et al., 2000; Yin et al., 1999), only about 31 ± 4% of GluA1-containing AMPARs were colocalized with GluA2 at the earlier E17/18 + 10DIV time point *vs.* 61 ± 2% by 13DIV (Suppl. Fig. 3, $p < 0.0006$), suggesting a predominance of GluA2-lacking AMPARs at this developmental stage, supported by *in vivo* observations in intact developing brain (Henley and Wilkinson, 2016). Combined with Ca^{2+} imaging, this suggests that GluA2-lacking CP-AMPARs in early life are poised to mediate activity-dependent Ca^{2+} signaling.

3.3. CP-AMPARs and LT-VGCCs mediate MeCP2 phosphorylation in E18 + 10DIV cell cultures

We next investigated the role of CP-AMPARs in activity-dependent MeCP2 phosphorylation *in vitro.* We predicted that elevated AMPAR-mediated Ca^{2+} influx at E18 + 10DIV, an age analogous to P10 in rodents or term to infancy in humans (Rakhade and Jensen, 2009), may provide age-specific seizure-induced hyperphosphorylation of MeCP2. We first used kainic acid (KA, 100 μM) stimulation to target ionotropic glutamate receptors and isolate the effects of upstream mediators on MeCP2 phosphorylation in E18 + 10DIV cultures (Suppl. Fig. 4). As in older (12DIV) cultures (Zhou et al., 2006), synaptic stimulation induced MeCP2 S421 phosphorylation in both cortical (Fig. 3A) and hippocampal neurons (Fig. 3B). However, unlike prior studies, 100 μM D-APV was not sufficient to prevent MeCP2 phosphorylation in DIV10 cortical neurons (Ctx: Fig. 3A: 76 ± 13% *vs.* KA, NaOH + DMSO treated controls, $p = 0.072$) or hippocampal neurons (H: Fig. 3B: 89 ± 13%, $p = 0.888$), suggesting that MeCP2 phosphorylation requires additional Ca^{2+} influx from alternate, non-NMDAR sources. In the presence of APV, MeCP2 phosphorylation was reduced by administration of either 50 μM NBQX (Ctx: Fig. 3A: 0 ± 0.3%, $p < 0.0001$; H: Fig. 3B: 3 ± 5%, $p < 0.0001$), or the CP-AMPAR antagonist NASPM (150 μM) (Ctx: 12 ± 2%, $p < 0.0001$; H: 30 ± 9%, $p < 0.0001$).

With respect to the relative efficacy of LT-VGCCs in MeCP2 S421 phosphorylation, we found that nimodipine (5 μM, with D-APV) also significantly decreased MeCP2

phosphorylation following KA-induced depolarization (Ctx: Fig. 3A: 4 ± 1%, $p < 0.0001$; H: Fig. 3B: 21 ± 6%, $p < 0.0001$). However, addition of nimodipine to D-APV and NASPM did not further decrease MeCP2 S421 phosphorylation in cortex ($p = 0.973$) and hippocampus ($p = 0.790$). Together, these findings suggest that both CP-AMPARs and LT-VGCCs each mediate essential Ca^{2+} influx to induce MeCP2 S421 phosphorylation in early life.

To examine the upstream mediators of Ca^{2+} influx in generalized neuronal depolarization, we stimulated neurons using high [KCl] and performed similar pharmacologic blockades as above. D-APV alone did not reverse KCl-mediated MeCP2 phoshorylation in cortical (Fig. 3C: 87 ± 21%, $p = 0.9637$) or hippocampal neurons (Fig. 3D: 73 ± 21%, $p = 0.373$). In contrast, phosphorylation was reduced (in the presence of D-APV) by NBQX (Ctx: Fig. 3C: 35 ± 5%, $p = 0.0215$; H: Fig. 3D: 21 ± 6%, $p = 0.0082$), NASPM (Ctx: Fig. 3C: 32 ± 13%, $p = 0.0241$; H: Fig. 3D: 11 ± 6%, $p = 0.0015$), and nimodipine (Ctx: Fig. 3C: 10 ± 6%, $p = 0.0005$; H: Fig. 3D: 0 ± 1%, $p = 0.0002$). Addition of nimodipine to NASPM and D-APV did not further reduce MeCP2 phosphorylation (Ctx: $p = 0.4352$; H: $p = 0.8012$). Overall, these results indicate that both CP-AMPARs and LT-VGCCs collectively contribute to MeCP2 S421 phosphorylation *via* two parallel pathways leading to depolarization-induced Ca^{2+} influx.

3.4. CaMKII T286 phosphorylation is upstream of MeCP2 phosphorylation and mediated by CP-AMPARs and LT-VGCCs in E18 + 10DIV cultures

Prior studies indicate that phosphorylation of MeCP2 S421 requires both CaMKII T286 phosphorylation and intracellular Ca^{2+} influx (Zhou et al., 2006), supported by our *in vivo* findings of sequential, seizure-induced activation of CaMKII and MeCP2 (Fig. 1). Consistent with these results, in both cortical (Fig. 4A) and hippocampal E18 + 10DIV cultures (Fig. 4B), phosphorylation of MeCP2 S421 was blocked by 5 μM KN93, a potent inhibitor of CaMKII (Ctx: 10 ± 3%, $p < 0.0001$; H: 3 ± 1%, $p < 0.0001$), but not its inactive form, KN92 (5 μM) (Ctx: 99 ± 3%, $p > 0.9999$; H: 97 ± 3%, $p > 0.9999$). Additionally, the Ca^{2+} chelator EGTA (1 mM) reduced phosphorylation of MeCP2 S421 (Ctx: 72 ± 7%, $p = 0.0005$; H: 66 ± 7%, $p < 0.0001$), as did the membrane-permeable form, 100 μM EGTA-AM in cortical (Fig. 4C: 64 ± 6%, $p = 0.0001$) and hippocampal (Fig. 4D: 53 ± 13%, $p = 0.0057$) neuronal cultures. Thus, CaMKII and intracellular Ca^{2+} regulate MeCP2 S421 phosphorylation at E18 + 10DIV.

As CaMKII is upstream of MeCP2 phosphorylation, we hypothesized that CaMKII pT286 required Ca^{2+} influx through the same channels as MeCP2 S421 phosphorylation. As with MeCP2, pre-treatment with D-APV did not fully reverse KA-induced CaMKII phosphorylation (Ctx: Fig. 5A: 81 ± 11%, $p = 0.2921$; H: Fig. 5B: 86 ± 9%, $p = 0.5213$). However, CaMKII phosphorylation was significantly reduced (in the presence of D-APV) with the addition of NBQX (Ctx: Fig. 5A: 18 ± 4%, $p < 0.0001$; H: Fig. 5B: 21 ± 3%, $p < 0.0001$), NASPM, (Ctx: Fig. 5A: 25 ± 5%, $p = 0.0001$; H: Fig. 5B: 28 ± 7%, $p < 0.0001$), and nimodipine (Ctx: Fig. 5A: 23 ± 9%, $p = 0.0002$; H: Fig. 5B: 33 ± 6%, $p < 0.0001$). However, LT-VGCC blockade did not reduce CaMKII T286 phosphorylation more than NASPM + D-APV alone (Ctx: $p = 0.7365$; H: $p = 0.929$). These results demonstrate that Ca^{2+} entry through both CP-AMPARs and LT-VGCCs contribute to activity-dependent

CaMKII T286 phosphorylation in immature cortical and hippocampal neurons, consistent with the effects on MeCP2 S421 phosphorylation.

3.5. In vivo HS-induced phosphorylation of MeCP2 S421 is prevented by AMPAR and LT-VGCC blockade

We previously showed that post-seizure *in vivo* treatment with NBQX prevents later-life seizures, altered synaptic plasticity, and autistic-like social deficits (Lippman-Bell et al., 2013; Zhou et al., 2011), whereas NMDAR antagonists do not prevent consequences of HS at this developmental time point (Jensen et al., 1995; Jensen and Wang, 1996). Given the *in vitro* evidence for CP-AMPARs in dysregulating MeCP2, we examined the effects of NBQX and the systemically administrable CP-AMPAR-specific inhibitor IEM-1460 (Szczurowska and Mares, 2015) on MeCP2 S421 phosphorylation *in vivo,* immediately after HS. Consistent with our prior *in vivo* post-HS outcomes (Lippman-Bell et al., 2013, 2016; Rakhade et al., 2008), administration of either 20 mg/kg NBQX or 20 mg/kg IEM-1460 (i.p.) (Magazanik et al., 1997; Szczurowska and Mares, 2015) significantly attenuated the increased MeCP2 S421 phosphorylation 3 h post-HS (Fig. 6: Control(C) + Vehicle (V) 100 ± 8%, HS + V 157 ± 11% normalized to mean C + V control, HS + NBQX 81 ± 8%, HS + IEM-1460 106 ± 11%; ANOVA $p = 0.002$, with post-hoc Tukey's comparisons: C + V *vs.* HS + V $p = 0.0003$, HS + V *vs.* HS + NBQX $p < 0.0001$, HS + V *vs.* HS + IEM-1460 $p = 0.0099$). We additionally confirmed that IEM-1460 reduced activity-dependent MeCP2 phosphorylation in cultured neurons *in vitro* cortical (Fig. 4C: 76 ± 5%, $p = 0.0039$) and hippocampal (Fig. 4D: 70 ± 8%, $p = 0.0361$) cell cultures. Paralleling our *in vitro* results, *in vivo* treatment with nimodipine reduced post-HS MeCP2 phosphorylation at 10 mg/kg, i.p. (Fig. 6: HS + NIMO 103 ± 9%, HS + V *vs.* HS + NIMO $p = 0.0051$), but not at a previously reported anti-convulsive dose of 5 mg/kg i.p. (Suppl. Fig. 5B) (Radzicki et al., 2013; Shitak et al., 2006, 2007). *In vivo* NBQX, IEM-1460, and nimodipine administration did not affect baseline MeCP2 phosphorylation in control rats (Suppl. Fig. 5A, B). Collectively, our *in vivo* findings support a critical role for CP-AMPARs and LT-VGCCs in mediating seizure-induced MeCP2 phosphorylation during early development.

4. Discussion

In early life, both seizures and autism share a developmental dysregulation of synaptogenesis and destabilized synaptic function, representing a potential overlap of underlying cellular mechanisms (Eichler and Meier, 2008). Early-life seizures contribute to later-life epilepsy and associated autistic-like behavioral deficits (Lippman-Bell et al., 2013; Talos et al., 2012), and epilepsy and autism often co-occur in neurodevelopmental disorders such as Rett Syndrome (Moretti et al., 2005; Neul et al., 2010; Pobbe et al., 2012; Tuchman, 2013). These findings suggest that seizures may dysregulate development in part through key activity-dependent neurodevelopmental signaling molecules implicated in ASDs, such as MeCP2. As neuronal activity modulates MeCP2 S421 function (Zhou et al., 2006), and neonatal seizures disrupt CP-AMPAR signaling (Rakhade et al., 2008; Sanchez et al., 2001; Zhou et al., 2011), the primary aim of this study was to determine if early-life seizures perturb MeCP2 through activation of Ca^{2+} *via* CP-AMPARs. We discovered that neonatal seizures elevate MeCP2 S421 phosphorylation *in vivo* 3 h post-seizure, and increase

CaMKII T286 phosphorylation 1 h post-seizure. Furthermore, both Ca^{2+} -permeable AMPARs and LT-VGCCs mediated a NMDAR-insensitive component of activity-dependent MeCP2 phosphorylation (Zhou et al., 2006).

Our findings that HS induce MeCP2 S421 phosphorylation align with prior reports of elevated MeCP2 S421 phosphorylation following kainic acid (KA)-induced seizure (Tao et al., 2009), pentylenetetrazole (PTZ)-induced seizure (Zhou et al., 2006), LTP-like high frequency stimulation (2 × 100 Hz, 20 s interval) (Li et al., 2011), and bicuculline stimulation (Buchthal et al., 2012), as well as psychostimulant-induced plasticity (Deng et al., 2010, 2014). Furthermore, out of four identified activity-dependent sites of MeCP2 phosphorylation, only S421 was elevated in the slowly migrating western blot band following kainic acid-induced seizures in rats (Tao et al., 2009), suggesting that S421 phosphorylation may represent a unique mediator of seizure-induced plasticity in rats. While some studies noted seizure-induced MeCP2 S421 phosphorylation as early as 30min to 1 h post seizure (Buchthal et al., 2012; Zhou et al., 2006), we note peak changes at the 3h time point, which may reflect experimental differences using our somewhat milder, yet physiologically relevant induction protocol (15 min hypoxia *vs.* chemoconvulsants). To our knowledge, our study is the first to examine a prolonged time course of early life seizure-induced MeCP2 phosphorylation up to 24 h, therefore we do not know in prior studies whether or when the phosphorylation returned to baseline.

Similar to the current study, we also previously observed sequential changes in other activity-dependent kinases after HS, with elevated CaMKII, PKA, and PKC activity at 1 h post-HS (Rakhade et al., 2008), and successive activation of members of the mTOR pathway (e.g. pERK/pAKT at 3h, p-p70S6 kinase at 12 h, pS6 kinase at 24 h) (Talos et al., 2012). Thus, HS likely produce multifocal, transient effects on many signaling pathways, with MeCP2 as one potential (but not exclusive) target for blockade. As many of these canonical signaling pathways are essential for proper synapse development and plasticity, we propose that even transient HS during the critical period may dysregulate these conduits (e.g. CaMKII, mTOR, MeCP2), which may in turn disrupt later-life cognition. Consistent with this idea, early-life impairments in MeCP2 function can disrupt visual critical period plasticity, leading to chronic deficits (He et al., 2014; Krishnan et al., 2015). In future studies, it would be valuable to know if acute or chronic blockade of MeCP2 S421 phosphorylation (e.g. phosphomutant $MeCP2^{S421A}$ mice (Cohen et al., 2011)) prevent later-life cognitive deficits or spontaneous seizure development following early-life HS (Koh et al., 2004; Lippman-Bell et al., 2013; Rakhade et al., 2011; Talos et al., 2012). We would predict that decreasing the level of S421 phosphorylation would rescue seizure-induced behavioral deficits, however it is a delicate balance; rendering S421 completely nonfunctional impairs social preference for novelty in a similar fashion to what we have seen following early-life HS (Cohen et al., 2011).

Neurons with elevated MeCP2 S421 phosphorylation share some phenotypic overlap with the MeCP2 KO *hypomorph* condition, as both demonstrate elevated expression of downstream transcriptional targets such as *BDNF in vitro* (Chen et al., 2003; Martinowich et al., 2003; Zhou et al., 2006). However, other studies *in vivo* demonstrate reduced *BDNF* expression in MeCP2 KO mice *vs.* WT (Chang et al., 2006), perhaps attributable to reduced

network activity in MeCP2 KO mice (Dani et al., 2005). Further, newer reports suggest that MeCP2 can serve as a transcriptional activator (Chahrour et al., 2008; Chang et al., 2006) and global chromatin regulator (Cohen et al., 2011) in addition to a repressor (Chen et al., 2003; Zhou et al., 2006), indicating that MeCP2 phosphorylation changes acquired as a result of seizures may have far reaching, unpredictable effects on downstream immediate early gene and neurotrophin expression. Future studies are warranted to examine how seizure-induced elevated MeCP2 S421 phosphorylation regulate target genes and signaling pathways *in vivo*.

We identified two novel, age-specific targets of seizure-induced MeCP2 S421 phosphorylation *in vitro* and *in vivo:* CP-AMPARs and LT-VGCCs. Elevated CP-AMPAR expression during early life (Rakhade and Jensen, 2009) not only contributes to the synaptic plasticity needed for synaptic refinement, but also likely provokes the progression of epileptogenesis (Rakhade and Jensen, 2009; Talos et al., 2006b), as NBQX, but not NMDAR antagonists, prevents increased seizure susceptibility following HS at P10 (Jensen et al., 1995; Jensen and Wang, 1996). To examine the mechanisms underlying activity-dependent activation of CP-AMPARs in early life, we used E18 + 10DIV cultured neurons, which express a high level of CP-AMPARs and MeCP2 (Yin et al., 1999). Unlike previous studies suggesting a dominance of NMDAR-mediated MeCP2 phosphorylation in older (E18 + 12DIV) neuronal cultures (Zhou et al., 2006), we found that two days earlier, at E18 + 10DIV, CP-AMPARs contribute to synaptically driven Ca^{2+} influx for activity-dependent MeCP2 phosphorylation, as evidenced by NASPM and NBQX significantly blocking KA-induced Ca^{2+} influx above that of APV alone.

Our *in vitro* model provides two unique paradigms to study MeCP2 phosphorylation: kainic acid (KA)-induced stimulation of ionotropic glutamate receptors and high [KCl]-induced neuronal depolarization, to account for additional non-synaptic effects. This model attempts to recreate elevated excitability hours post hypoxic-seizures *in vivo* (Lippman-Bell et al., 2016; Rakhade et al., 2008), while avoiding acute effects due to hypoxia itself, such as primary changes in levels of ATP, adenosine, pH, and neurotransmitter release that precede later hyper-excitability (Di Filippo et al., 2008; Mukandala et al., 2016). The *in vitro* studies provide an assay to systematically and pharmacologically target the receptors and channels that mediate MeCP2 phosphorylation, however bath application of KA or KCl may not produce the same activation and time course as synaptically released glutamate *in vivo*. Therefore, we also demonstrate that both the AMPAR antagonist NBQX and the novel CP-AMPAR blocker IEM-1460 prevented seizure-induced MeCP2 phosphorylation *in vivo*, further underscoring the relevance of our *in vitro* model.

Additionally, *in vivo* blockade of LT-VGCCs *via* nimodipine at higher (10 mg/kg), but not lower (5 mg/kg) doses, reduced HS-induced MeCP2 phosphorylation. Our *in vitro* findings suggest that Ca^{2+} influx from LT-VGCCs and CP-AMPARs both individually contribute to MeCP2 phosphorylation, and both pathways likely converge on a common endpoint. Notably, LT-VGCCs are developmentally upregulated during early postnatal development (Kramer et al., 2012; Morton et al., 2013; Schlick et al., 2010), and have been implicated in promoting both epileptogenesis (Beck et al., 1998; Siwek et al., 2012; Speckmann et al., 1993; Stiglbauer et al., 2017) and ASD-like behavior (Jinnah et al., 1999); Ca^{2+} influx-

promoting mutations in LT-VGCCs cause Timothy Syndrome, a rare genetic form of ASD (Bader et al., 2011; Barrett and Tsien, 2008; Splawski et al., 2004).

Thus, both LT-VGCCs and CP-AMPARs appear to have a developmentally regulated, privileged role for MeCP2 S421 phosphorylation, even during a period when NMDARs contain an elevated NR2B:NR2A subunit ratio with transiently enhanced Ca^{2+} permeability, albeit with slower kinetics (Monyer et al., 1994; Yashiro and Philpot, 2008). In comparing the role of AMPARs and LT-VGCCs to seizure-induced MeCP2 phosphorylation, we recently found that NASPM, but not nimodipine or D-APV, limit elevated Ca^{2+} influx in acute hippocampal slices from rats post-HS at P10 (Lippman-Bell et al., 2016). Further studies may be required to fully understand the interactions between AMPARs and LT-VGCCs on MeCP2 S421 phosphorylation.

MeCP2 likely plays a pivotal role in regulating activity-dependent gene transcription important for neural function, maturation of spine density, neuronal connectivity, dendritic arborization, behavior (Cohen et al., 2011; Jiang et al., 2013; Kishi and Macklis, 2010; Luikenhuis et al., 2004; Mullaney et al., 2004; Shahbazian et al., 2002b; Zhou et al., 2006), and multple forms of synaptic plasticity, including synaptic scaling (Blackman et al., 2012; Qiu et al., 2012; Zhong et al., 2012) and Hebbian plasticity (Li et al., 2011; Moretti et al., 2006; Munoz et al., 2016; Weng et al., 2011). Mouse models of Rett Syndrome with decreased or blocked expression of MeCP2 show impaired LTP in area CA1 of the hippocampus (Asaka et al., 2006; Weng et al., 2011), changes in glutamate receptor expression including decreased NR2A (Asaka et al., 2006), behavioral deficits (Neul et al., 2010), and increased spontaneous seizure susceptibility (D'Cruz et al., 2010; Shahbazian et al., 2002a; Zhang et al., 2014). All of these changes also occur in an acquired manner in the HS neonatal seizure model (Bo et al., 2004; Lippman-Bell et al., 2013; Zhou et al., 2011), which we now show alters MeCP2 S421 phosphorylation. The phenotypic and molecular overlap between HS and MeCP2 KO mice raises the important possibility that seizures themselves impair synaptic function and may lead to later-life cognitive and behavioral deficits in part by dysregulating physiologic MeCP2 function in the immature brain.

Our study provides key evidence for AMPARs as an *upstream* mediator of MeCP2 phosphorylation, complementing prior findings of AMPARs as a key downstream component of MeCP2-mediated signaling. Indeed, GluA1 and GluA2 subunit trafficking is impaired both in LTP in MeCP2 KO mice (Li et al., 2016), and homeostatic synaptic scaling with MeCP2 knockdown (Blackman et al., 2012; Qiu et al., 2012). Taken together, these data suggest that AMPARs (along with LT-VGCCs) play a crucial role in a NMDAR-insensitive component of seizure-induced MeCP2-regulated signaling, which could in turn trigger later-life cognitive deficits or spontaneous seizures. Consistent with this hypothesis, IEM-1460 reduced hyperexcitability following both PTZ (Szczurowska and Mares, 2015) and pilocarpine-induced seizures (Malkin et al., 2016), and nimodipine prevented later-life impairments in spatial memory following PTZ kindling (Wang et al., 2008) as well as behavioral deficits after focal ischemic-reperfusion excitotoxicity (Babu and Ramanathan, 2011). Combined with prior knowledge that both CP-AMPARs (Fortin et al., 2010; Park et al., 2016) and LT-VGCCs (Da Silva et al., 2013; Grover and Teyler, 1990) play a key role in

some forms of synaptic plasticity, we predict that both of these targets will play an essential role in HS-induced cognitive deficits later in life.

HS-induced signaling through AMPARs and LT-VGCCs may also mediate changes in other proteins implicated in Rett Syndrome, such as CDKL5 (Tao et al., 2004; Weaving et al., 2004), which is known to be highly regulated by activity (Rusconi et al., 2011; Zhou et al., 2006). CDKL5 directly binds and phosphorylates MeCP2 *in vitro* and *in vivo* (Mari et al., 2005) and regulates dendritic morphology and synapse development (Chen et al., 2010; Mari et al., 2005; Zhou et al., 2006; Zhu et al., 2013), suggesting that they may share common signaling pathways. Future studies should address whether seizure-induced CaMKII-MeCP2 activation cooperates spatially and temporally with CDKL5-MeCP2 phosphorylation, and if these interactions are implicated in Rett Syndrome pathophysiology.

Collectively, we propose that the AMPAR-MeCP2 pathway, along with that of the LT-VGCCs, may provide a therapeutically targetable mechanism for post-HS long-term behavioral changes, presenting an exciting area of further research relating to the interaction between epilepsy and autism in early postnatal brain development.

5. Conclusions

In this study, we provide novel evidence that seizures in the wild-type early-life brain dysregulate MeCP2, a critical mediator of synaptic development that has been implicated in the ASD Rett Syndrome. Further, we demonstrate that systemically blocking Ca^{2+} -permeable AMPARs (CP-AMPARs) and LT-VGCCs, two targets overexpressed in the immature brain, reverses seizure-induced MeCP2 phosphorylation. Furthering our understanding of these age-specific molecular pathways will lead to improved treatments for both epilepsy and ASDs, and better elucidate the interaction between these disorders.

Supplementary Material

Refer to Web version on PubMed Central for supplementary material.

Acknowledgements

We thank D. Talos for helpful comments on the manuscript and M. Greenberg for antibodies.

Funding sources

This work was supported by NIH Grants NS 068161 (JJL), NS 031718 (FEJ), NS 080565 (FEJ), DP1 0D003347 (FEJ) (from the Office of the Director). The authors declare no conflict of interest.

Abbreviations:

MeCP2	methyl CpG binding protein 2
CP-AMPARs	calcium-permeable α-amino-3-hydroxy-5-methyl-4-isoxazolepropionic acid (AMPAR) receptors
NMDARs	*N*-methyl-D-aspartate receptor

LT-VGCCs	l-type voltage gated calcium channels
HS	hypoxic seizures
ASD	autism spectrum disorder
KCl	potassium chloride
KA	kainic acid
NBQX	2,3-dihydroxy-6-nitro-7-sulfamoyl-benzo[*f*]quinoxaline-2,3-dione
NASPM	1-Naphthyl acetyl spermine trihydrochloride
D-APV	D-(−)-2-Amino-5-phosphonopentanoic acid
Nimo	nimo-dipine

References

Aarts E, et al., 2014 A solution to dependency: using multilevel analysis to accommodate nested data. Nat. Neurosci. 17, 491–496. [PubMed: 24671065]

Amir RE, et al., 1999 Rett syndrome is caused by mutations in X-linked MECP2, encoding methyl-CpG-binding protein 2. Nat. Genet. 23, 185–188. [PubMed: 10508514]

Asaka Y, et al., 2006 Hippocampal synaptic plasticity is impaired in the Mecp2-null mouse model of Rett syndrome. Neurobiol. Dis. 21, 217–227. [PubMed: 16087343]

Babu CS, Ramanathan M, 2011 Post-ischemic administration of nimodipine following focal cerebral ischemic-reperfusion injury in rats alleviated excitotoxicity, neurobehavioural alterations and partially the bioenergetics. Int. J. Dev. Neurosci. 29, 93–105. [PubMed: 20713150]

Bader PL, et al., 2011 Mouse model of Timothy syndrome recapitulates triad of autistic traits. Proc. Natl. Acad. Sci. U. S. A. 108, 15432–15437. [PubMed: 21878566]

Barrett CF, Tsien RW, 2008 The Timothy syndrome mutation differentially affects voltage-and calcium-dependent inactivation of $Ca_V1.2$ L-type calcium channels. Proc. Natl. Acad. Sci. U. S. A. 105, 2157–2162. [PubMed: 18250309]

Beck H, et al., 1998 Voltage-dependent Ca2+ currents in epilepsy. Epilepsy Res. 32, 321–332. [PubMed: 9761331]

Bellini E, et al., 2014 MeCP2 post-translational modifications: a mechanism to control its involvement in synaptic plasticity and homeostasis? Front. Cell. Neurosci. 8, 236. [PubMed: 25165434]

Ben Ari Y, Holmes GL, 2006 Effects of seizures on developmental processes in the immature brain. Lancet Neurol. 5, 1055–1063. [PubMed: 17110286]

Berg AT, et al., 2011 Risk and correlates of autism spectrum disorder in children with epilepsy: a community-based study. J. Child Neurol. 26, 540–547. [PubMed: 21421903]

Blackman MP, et al., 2012 A critical and cell-autonomous role for MeCP2 in synaptic scaling up. J. Neurosci. 32, 13529–13536. [PubMed: 23015442]

Bo T, et al., 2004 Long-term effects of seizures in neonatal rats on spatial learning ability and N-methyl-D-aspartate receptor expression in the brain. Brain Res. Dev. Brain Res. 152, 137–142. [PubMed: 15351501]

Brooks-Kayal A, 2010 Epilepsy and autism spectrum disorders: are there common developmental mechanisms? Brain and Development 32, 731–738. [PubMed: 20570072]

Brooks-Kayal A, 2011 Molecular mechanisms of cognitive and behavioral comorbidities of epilepsy in children. Epilepsia 52, 13–20.

Buchthal B, et al., 2012 Nuclear calcium signaling controls methyl-CpG-binding protein 2 (MeCP2) phosphorylation on serine 421 following synaptic activity. J. Biol. Chem. 287, 30967–30974. [PubMed: 22822052]

Castelhano AS, et al., 2013 Altered anxiety-related and abnormal social behaviors in rats exposed to early life seizures. Front. Behav. Neurosci. 7, 36. [PubMed: 23675329]

Chahrour M, et al., 2008 MeCP2, a key contributor to neurological disease, activates and represses transcription. Science 320, 1224–1229. [PubMed: 18511691]

Chang YC, et al., 2003 Febrile seizures impair memory and cAMP response-element binding protein activation. Ann. Neurol. 54, 706–718. [PubMed: 14681880]

Chang Q, et al., 2006 The disease progression of Mecp2 mutant mice is affected by the level of BDNF expression. Neuron 49, 341–348. [PubMed: 16446138]

Chen WG, et al., 2003 Derepression of BDNF transcription involves calcium-dependent phosphorylation of MeCP2. Science 302, 885–889. [PubMed: 14593183]

Chen Q, et al., 2010 CDKL5, a protein associated with rett syndrome, regulates neuronal morphogenesis via Racl signaling. J. Neurosci. 30, 12777–12786. [PubMed: 20861382]

Cohen S, et al., 2011 Genome-wide activity-dependent MeCP2 phosphorylation regulates nervous system development and function. Neuron 72, 72–85. [PubMed: 21982370]

Cull-Candy S, et al., 2006 Regulation of Ca2+ -permeable AMPA receptors: synaptic plasticity and beyond. Curr. Opin. Neurobiol. 16, 288–297. [PubMed: 16713244]

Da Silva WC, et al., 2013 Memory reconsolidation and its maintenance depend on L-voltage-dependent calcium channels and CaMKII functions regulating protein turnover in the hippocampus. Proc. Natl. Acad. Sci. U. S. A. 110, 6566–6570. [PubMed: 23576750]

Dani VS, et al., 2005 Reduced cortical activity due to a shift in the balance between excitation and inhibition in a mouse model of Rett syndrome. Proc. Natl. Acad. Sci. U. S. A. 102, 12560–12565. [PubMed: 16116096]

D'Cruz JA, et al., 2010 Alterations of cortical and hippocampal EEG activity in MeCP2-deficient mice. Neurobiol. Dis. 38, 8–16. [PubMed: 20045053]

Deng JV, et al., 2010 MeCP2 in the nucleus accumbens contributes to neural and behavioral responses to psychostimulants. Nat. Neurosci. 13, 1128–1136. [PubMed: 20711186]

Deng JV, et al., 2014 MeCP2 phosphorylation limits psychostimulant-induced behavioral and neuronal plasticity. J. Neurosci. 34, 4519–4527. [PubMed: 24671997]

Di Filippo M, et al., 2008 Plasticity and repair in the post-ischemic brain. Neuropharmacology 55, 353–362. [PubMed: 18359495]

Dube CM, et al., 2009 Cognitive dysfunction after experimental febrile seizures. Exp. Neurol. 215, 167–177. [PubMed: 19000675]

Eichler SA, Meier JC, 2008 E-I balance and human diseases - from molecules to networking. Front. Mol. Neurosci. 1, 2. [PubMed: 18946535]

Feldman D, et al., 2016 Developmental dynamics of Rett syndrome. Neural Plast. 2016, 6154080.

Fortin DA, et al., 2010 Long-term potentiation-dependent spine enlargement requires synaptic Ca2+ -permeable AMPA receptors recruited by CaM-kinase I. J. Neurosci. 30, 11565–11575. [PubMed: 20810878]

Glass HC, Ferriero DM, 2007 Treatment of hypoxic-ischemic encephalopathy in newborns. Curr. Treat. Options Neurol. 9, 414–423. [PubMed: 18173941]

Grover LM, Teyler TJ, 1990 Two components of long-term potentiation induced by different patterns of afferent activation. Nature 347, 477–479. [PubMed: 1977084]

He LJ, et al., 2014 Conditional deletion of Mecp2 in parvalbumin-expressing GABAergic cells results in the absence of critical period plasticity. Nat. Commun. 5, 5036. [PubMed: 25297674]

Henley JM, Wilkinson KA, 2016 Synaptic AMPA receptor composition in development, plasticity and disease. Nat. Rev. Neurosci. 17, 337–350. [PubMed: 27080385]

Hernan AE, et al., 2013 Altered short-term plasticity in the prefrontal cortex after early life seizures. Neurobiol. Dis. 50, 120–126. [PubMed: 23064435]

Holmes GL, et al., 1998 Consequences of neonatal seizures in the rat: morphological and behavioral effects. Ann. Neurol. 44, 845–857. [PubMed: 9851428]

Huang LT, et al., 2002 Pentylenetetrazol-induced recurrent seizures in rat pups: time course on spatial learning and long-term effects. Epilepsia 43, 567–573. [PubMed: 12060014]

Hughes EG, et al., 2010 Cellular and synaptic mechanisms of anti-NMDA receptor encephalitis. J. Neurosci. 30, 5866–5875. [PubMed: 20427647]

Isaeva E, et al., 2013 Alteration of synaptic plasticity by neonatal seizures in rat somatosensory cortex. Epilepsy Res. 106, 280–283. [PubMed: 23623846]

Jensen FE, 2009 Neonatal seizures: an update on mechanisms and management. Clin. Perinatol. 36, 881–900 (vii). [PubMed: 19944840]

Jensen FE, Wang C, 1996 Hypoxia-induced hyperexcitability in vivo and in vitro in the immature hippocampus. Epilepsy Res. 26 (1), 131–140. [PubMed: 8985695]

Jensen FE, et al., 1992 Age dependent changes in long term seizure susceptibility and behavior after hypoxia in rats. Epilepsia 33, 971–980. [PubMed: 1464280]

Jensen FE, et al., 1995 NBQX blocks acute and late epileptogenic effects of perinatal hypoxia. Epilepsia 36, 966–972. [PubMed: 7555960]

Jiang M, et al., 2013 Dendritic arborization and spine dynamics are abnormal in the mouse model of MECP2 duplication syndrome. J. Neurosci. 33, 19518–19533. [PubMed: 24336718]

Jinnah HA, et al., 1999 Calcium channel activation and self-biting in mice. Proc. Natl. Acad. Sci. U. S. A. 96, 15228–15232. [PubMed: 10611367]

Kishi N, Macklis JD, 2010 MeCP2 functions largely cell-autonomously, but also non-cell-autonomously, in neuronal maturation and dendritic arborization of cortical pyramidal neurons. Exp. Neurol. 222, 51–58. [PubMed: 20025874]

Koh S, et al., 2004 NBQX or topiramate treatment after perinatal hypoxia-induced seizures prevents later increases in seizure-induced neuronal injury. Epilepsia 45, 569–575. [PubMed: 15144420]

Kramer AA, et al., 2012 Levels of Ca(V)1.2 L-type Ca(2+) channels peak in the first two weeks in rat hippocampus whereas Ca(V)1.3 channels steadily increase through development. J. Signal Transduct. 2012, 597214.

Krishnan K, et al., 2015 MeCP2 regulates the timing of critical period plasticity that shapes functional connectivity in primary visual cortex. Proc. Natl. Acad. Sci. U. S. A. 112, E4782–91.

Kumar SS, et al., 2002 A developmental switch of AMPA receptor subunits in neo-cortical pyramidal neurons. J. Neurosci. 22, 3005–3015. [PubMed: 11943803]

Li H, et al., 2011 Loss of activity-induced phosphorylation of MeCP2 enhances synaptogenesis, LTP and spatial memory. Nat. Neurosci. 14 (8), 1001. [PubMed: 21765426]

Li W, et al., 2016 Excitatory synapses are stronger in the hippocampus of Rett syndrome mice due to altered synaptic trafficking of AMPA-type glutamate receptors. Proc. Natl. Acad. Sci. U. S. A. 113, E1575–84.

Lippman-Bell JJ, et al., 2013 AMPA receptor antagonist NBQX attenuates later-life epileptic seizures and autistic-like social deficits following neonatal seizures. Epilepsia 54, 1922–1932. [PubMed: 24117347]

Lippman-Bell JJ, et al., 2016 Early-life seizures alter synaptic calcium-permeable AMPA receptor function and plasticity. Mol. Cell. Neurosci. 76, 11–20. [PubMed: 27521497]

Lucas MM, et al., 2011 Impaired cognition in rats with cortical dysplasia: additional impact of early-life seizures. Brain 134, 1684–1693. [PubMed: 21602270]

Lugo JN, et al., 2014 Early-life seizures result in deficits in social behavior and learning. Exp. Neurol. 256, 74–80. [PubMed: 24685665]

Luikenhuis S, et al., 2004 Expression of MeCP2 in postmitotic neurons rescues Rett syndrome in mice. Proc. Natl. Acad. Sci. U. S. A. 101, 6033–6038. [PubMed: 15069197]

Magazanik LG, et al., 1997 Block of open channels of recombinant AMPA receptors and native AMPA/kainate receptors by adamantane derivatives. J. Physiol. 505 (Pt 3), 655–663. [PubMed: 9457643]

Malkin SL, et al., 2016 Changes of AMPA receptor properties in the neocortex and hippocampus following pilocarpine-induced status epilepticus in rats. Neuroscience 327, 146–155. [PubMed: 27109923]

Mari F, et al., 2005 CDKL5 belongs to the same molecular pathway of MeCP2 and it is responsible for the early-onset seizure variant of Rett syndrome. Hum. Mol. Genet. 14, 1935–1946. [PubMed: 15917271]

Martinowich K, et al., 2003 DNA methylation-related chromatin remodeling in activity-dependent BDNF gene regulation. Science 302, 890–893. [PubMed: 14593184]

Minchom P, et al., 1987 Antecedents and outcome of very early neonatal seizures in infants born at or after term. Br. J. Obstet. Gynaecol. 94, 431–439. [PubMed: 3580326]

Monyer H, et al., 1994 Developmental and regional expression in the rat brain and functional properties of four NMDA receptors. Neuron 12, 529–540. [PubMed: 7512349]

Moretti P, et al., 2005 Abnormalities of social interactions and home-cage behavior in a mouse model of Rett syndrome. Hum. Mol. Genet. 14, 205–220. [PubMed: 15548546]

Moretti P, et al., 2006 Learning and memory and synaptic plasticity are impaired in a mouse model of Rett syndrome. J. Neurosci. 26, 319–327. [PubMed: 16399702]

Morton RA, et al., 2013 Characterization of L-type voltage-gated Ca(2+) channel expression and function in developing CA3 pyramidal neurons. Neuroscience 238, 59–70. [PubMed: 23415785]

Mukandala G, et al., 2016 The effects of hypoxia and inflammation on synaptic signaling in the CNS. Brain Sci. 6.

Mullaney BC, et al., 2004 Developmental expression of methyl-CpG binding protein 2 is dynamically regulated in the rodent brain. Neuroscience 123, 939–949. [PubMed: 14751287]

Munoz P, et al., 2016 Inhibition of DNA methylation impairs synaptic plasticity during an early time window in rats. Neural Plast. 2016, 4783836.

Neul JL, et al., 2010 Rett syndrome: revised diagnostic criteria and nomenclature. Ann. Neurol. 68, 944–950. [PubMed: 21154482]

Park P, et al., 2016 Calcium-permeable AMPA receptors mediate the induction of the protein kinase A-dependent component of long-term potentiation in the hippocampus. J. Neurosci. 36, 622–631. [PubMed: 26758849]

Pickard L, et al., 2000 Developmental changes in synaptic AMPA and NMDA receptor distribution and AMPA receptor subunit composition in living hippocampal neurons. J. Neurosci. 20, 7922–7931. [PubMed: 11050112]

Pobbe RL, et al., 2012 Oxytocin receptor and Mecp2 308/Y knockout mice exhibit altered expression of autism-related social behaviors. Physiol. Behav. 107, 641–648. [PubMed: 22406388]

Qiu Z, et al., 2012 The Rett syndrome protein MeCP2 regulates synaptic scaling. J. Neurosci. 32, 989–994. [PubMed: 22262897]

Radzicki D, et al., 2013 Temperature-sensitive Cav1.2 calcium channels support intrinsic firing of pyramidal neurons and provide a target for the treatment of febrile seizures. J. Neurosci. 33, 9920–9931. [PubMed: 23761887]

Rakhade SN, Jensen FE, 2009 Epileptogenesis in the immature brain: emerging mechanisms. Nat. Rev. Neurol. 5, 380–391. [PubMed: 19578345]

Rakhade SN, et al., 2008 Early alterations of AMPA receptors mediate synaptic potentiation induced by neonatal seizures. J. Neurosci. 28, 7979–7990. [PubMed: 18685023]

Rakhade SN, et al., 2011 Development of later life spontaneous seizures in a rodent model of hypoxia-induced neonatal seizures. Epilepsia 52, 753–765. [PubMed: 21366558]

Rakhade SN, et al., 2012 Glutamate receptor 1 phosphorylation at serine 831 and 845 modulates seizure susceptibility and hippocampal hyperexcitability after early life seizures. J. Neurosci. 32, 17800–17812. [PubMed: 23223299]

Rusconi L, et al., 2011 Extrasynaptic N-methyl-D-aspartate (NMDA) receptor stimulation induces cytoplasmic translocation of the CDKL5 kinase and its proteasomal degradation. J. Biol. Chem. 286, 36550–36558. [PubMed: 21832092]

Sanchez RM, et al., 2001 Decreased glutamate receptor 2 expression and enhanced epileptogenesis in immature rat hippocampus after perinatal hypoxia-induced seizures. J. Neurosci. 21, 8154–8163. [PubMed: 11588188]

Sayin U, et al., 2004 Seizures in the developing brain cause adverse long-term effects on spatial learning and anxiety. Epilepsia 45, 1539–1548. [PubMed: 15571512]

Schlick B, et al., 2010 Voltage-activated calcium channel expression profiles in mouse brain and cultured hippocampal neurons. Neuroscience 167, 786–798. [PubMed: 20188150]

Shahbazian M, et al., 2002a Mice with truncated MeCP2 recapitulate many Rett syndrome features and display hyperacetylation of histone H3. Neuron 35, 243–254. [PubMed: 12160743]

Shahbazian MD, et al., 2002b Insight into Rett syndrome: MeCP2 levels display tissue-and cell-specific differences and correlate with neuronal maturation. Hum. Mol. Genet. 11, 115–124. [PubMed: 11809720]

Shitak R, et al., 2006 Anti-seizure efficacy of nimodipine in pentylenetetrazole and kainic acid combined seizure models in mice. Indian J. Physiol. Pharmacol. 50, 265–272. [PubMed: 17193898]

Shitak R, et al., 2007 Evaluation of the modulatory role of nimodipine in seizures induced by kainic acid and pentylenetetrazole in mice. Methods Find. Exp. Clin. Pharmacol. 29, 11–17. [PubMed: 17344939]

Siwek M, et al., 2012 Voltage-gated Ca(2+) channel mediated Ca(2+) influx in epi-leptogenesis. Adv. Exp. Med. Biol. 740, 1219–1247. [PubMed: 22453990]

Speckmann EJ, et al., 1993 Contribution of calcium ions to the generation of epileptic activity and antiepileptic calcium antagonism. Neuropsychobiology 27, 122–126. [PubMed: 8232825]

Splawski I, et al., 2004 Ca(V)1.2 calcium channel dysfunction causes a multisystem disorder including arrhythmia and autism. Cell 119, 19–31. [PubMed: 15454078]

Stiglbauer V, et al., 2017 Cav 1.3 channels play a crucial role in the formation of paroxysmal depolarization shifts in cultured hippocampal neurons. Epilepsia 58, 858–871. [PubMed: 28295232]

Swann JW, 2004 The effects of seizures on the connectivity and circuitry of the developing brain. Ment. Retard. Dev. Disabil. Res. Rev. 10, 96–100. [PubMed: 15362163]

Szczurowska E, Mares P, 2015 An antagonist of calcium permeable AMPA receptors, IEM1460: anticonvulsant action in immature rats? Epilepsy Res. 109, 106–113. [PubMed: 25524849]

Talos D, et al., 2006a Developmental regualtion of alpha-amino-3-hydroxy-5-methyl-4-isoxazole-proprionic acid receptor subunit expression in forebrain and relationship to regional susceptibility to hypoxic/ischemic injury. I. Rodent cerebral white matter and cortex. J. Comp. Neurol. 497, 42–61. [PubMed: 16680782]

Talos D, et al., 2006b Developmental regualtion of alpha-amino-3-hydroxy-5-methyl-4-isoxazole-proprionic acid receptor subunit expression in forebrain and relationship to regional susceptibility to hypoxic/ischemic injury. II. Human cerebral white matter and cortex. J. Comp. Neurol. 497, 61–77. [PubMed: 16680761]

Talos DM, et al., 2012 The interaction between early life epilepsy and autistic-like behavioral consequences: a role for the mammalian target of rapamycin (mTOR) pathway. PLoS One 7, e35885.

Tao J, et al., 2004 Mutations in the X-linked cyclin-dependent kinase-like 5 (CDKL5/STK9) gene are associated with severe neurodevelopmental retardation. Am. J. Hum. Genet. 75, 1149–1154. [PubMed: 15499549]

Tao J, et al., 2009 Phosphorylation of MeCP2 at Serine 80 regulates its chromatin association and neurological function. Proc. Natl. Acad. Sci. U. S. A. 106, 4882–4887. [PubMed: 19225110]

Tekgul H, et al., 2006 The current etiologic profile and neurodevelopmental outcome of seizures in term newborn infants. Pediatrics 117, 1270–1280. [PubMed: 16585324]

Tuchman R, 2013 Autism and social cognition in epilepsy: implications for comprehensive epilepsy care. Curr. Opin. Neurol. 26, 214–218. [PubMed: 23400237]

Wang P, et al., 2008 Impaired spatial learning related with decreased expression of calcium/calmodulin-dependent protein kinase IIalpha and cAMP-response element binding protein in the pentylenetetrazol-kindled rats. Brain Res. 1238, 108–117. [PubMed: 18710651]

Wang IT, et al., 2012 Loss of CDKL5 disrupts kinome profile and event-related potentials leading to autistic-like phenotypes in mice. Proc. Natl. Acad. Sci. U. S. A. 109, 21516–21521. [PubMed: 23236174]

Weaving LS, et al., 2004 Mutations of CDKL5 cause a severe neurodevelopmental disorder with infantile spasms and mental retardation. Am. J. Hum. Genet. 75, 1079–1093. [PubMed: 15492925]

Weng SM, et al., 2011 Synaptic plasticity deficits in an experimental model of rett syndrome: long-term potentiation saturation and its pharmacological reversal. Neuroscience 180, 314–321. [PubMed: 21296130]

Wirrell EC, et al., 2011 Incidence and classification of new-onset epilepsy and epilepsy syndromes in children in Olmsted County, Minnesota from 1980 to 2004: a population-based study. Epilepsy Res. 95, 110–118. [PubMed: 21482075]

Xia Y, et al., 1996 Nitric oxide synthase generates superoxide and nitric oxide in arginine-depleted cells leading to peroxynitrite-mediated cellular injury. Proc. Natl. Acad. Sci. U. S. A. 93, 6770–6774. [PubMed: 8692893]

Yashiro K, Philpot BD, 2008 Regulation of NMDA receptor subunit expression and its implications for LTD, LTP, and metaplasticity. Neuropharmacology 55, 1081–1094. [PubMed: 18755202]

Yin HZ, et al., 1999 Dendritic localization of Ca(2+)-permeable AMPA/kainate channels in hippocampal pyramidal neurons. J. Comp. Neurol. 409, 250–260. [PubMed: 10379918]

Zhang W, et al., 2014 Loss of MeCP2 from forebrain excitatory neurons leads to cortical hyperexcitation and seizures. J. Neurosci. 34, 2754–2763. [PubMed: 24523563]

Zhong X, et al., 2012 MeCP2 phosphorylation is required for modulating synaptic scaling through mGluR5. J. Neurosci. 32, 12841–12847. [PubMed: 22973007]

Zhou Z, et al., 2006 Brain-specific phosphorylation of MeCP2 regulates activity-dependent Bdnf transcription, dendritic growth, and spine maturation. Neuron 52, 255–269. [PubMed: 17046689]

Zhou C, et al., 2011 Hypoxia-induced neonatal seizures diminish silent synapses and long-term potentiation in hippocampal CA1 neurons. J. Neurosci. 13, 18211–18222.

Zhu YC, et al., 2013 Palmitoylation-dependent CDKL5-PSD-95 interaction regulates synaptic targeting of CDKL5 and dendritic spine development. Proc. Natl. Acad. Sci. U. S. A. 110, 9118–9123. [PubMed: 23671101]

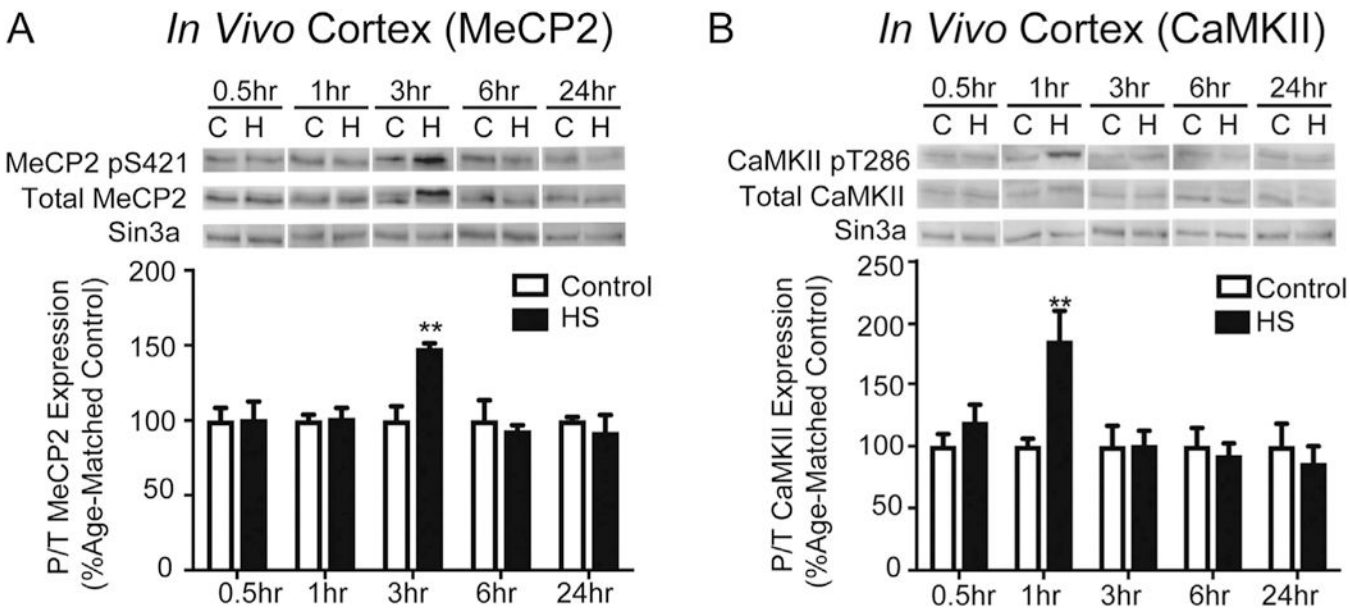

Fig. 1.

Hypoxic seizures (HS) in P10 rats induce phosphorylation of MeCP2 S421 and CaMKII T286 in cortex. (A) Increased MeCP2 S421 phosphorylation at 3 h postseizure induction (n = 4 samples/group with 3 rat cortices pooled for one sample, p = 0.003) and (B) increased CaMKII T286 phosphorylation at 1 h post-seizure (n = 4, p = 0.009). C = normoxic controls, HS = post-seizure rats. For all figures, error bars represent standard error of mean. *p < 0.05, **p < 0.1, ***p < 0.001, ****p < 0.0001.

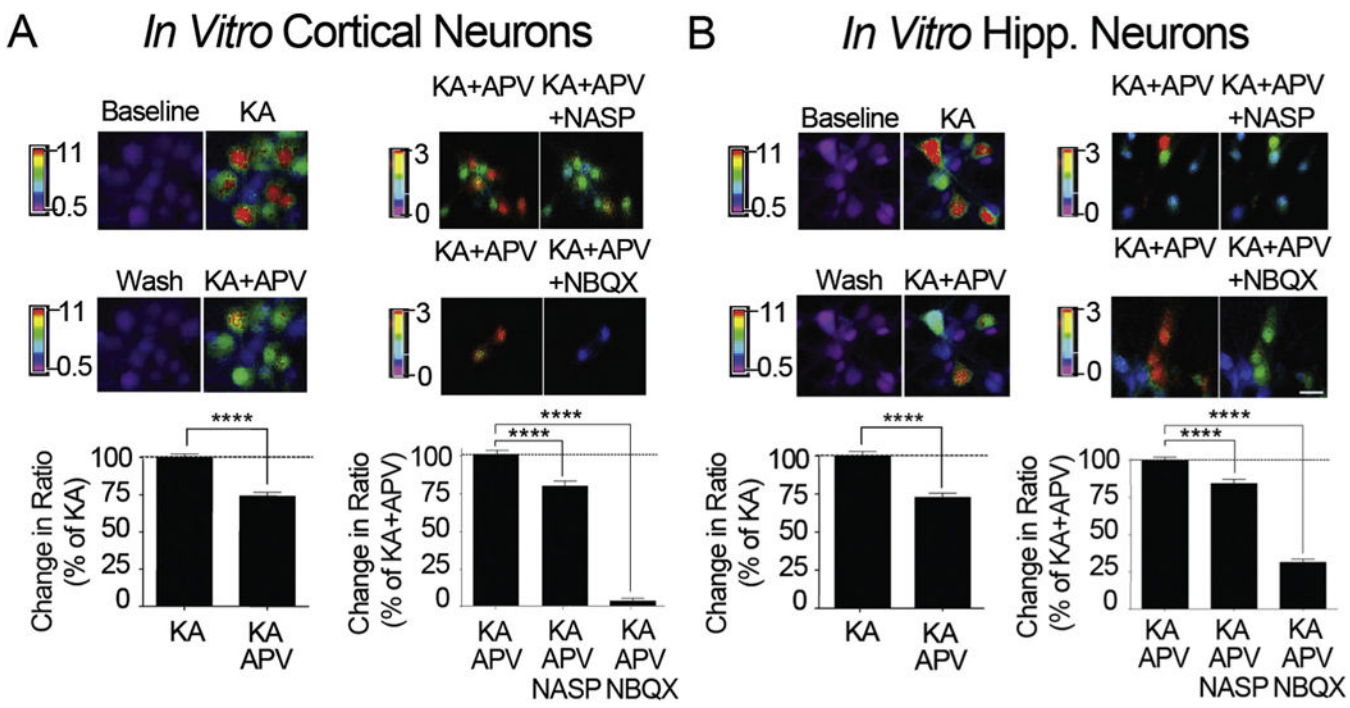

Fig. 2.

AMPARs mediate kainic acid (KA)-induced Ca^{2+} influx in E18 + 10DIV cortical and hippocampal neuronal cultures. Kainic acid (KA)-induced Ca^{2+} influx in Fura-2 loaded neurons decreased following incubation with the NMDAR antagonist D-APV in C = cortical (A, KA + APV *vs.* KA, n = 104 cells from 2 coverslips, $p < 0.0001$) and (B) H=hippocampal neuronal cultures (KA + APV *vs.* KA, n = 68 cells from 3 coverslips, $p < 0.0001$). Bar graphs represent mean peak 340/380 excitation ratio, normalized to average of KA condition. NMDAR-sensitive Ca^{2+} influx was further decreased by both the AMPAR antagonist NBQX (KA + APV + NBQX, C: n = 102 cells from 3 coverslips; H: n = 133 cells from 5 coverslips; $p < 0.0001$ for both) and NASPM, a blocker of Ca^{2+} permeable AMPARs (KA + APV + NASPM, C: n = 133 cells from 3 coverslips; H: n = 176 cells from 6 coverslips, $p < 0.0001$ for both), normalized to average of KA + APV condition. Ratiometric scales are left of each set, scale bar = 20 μm.

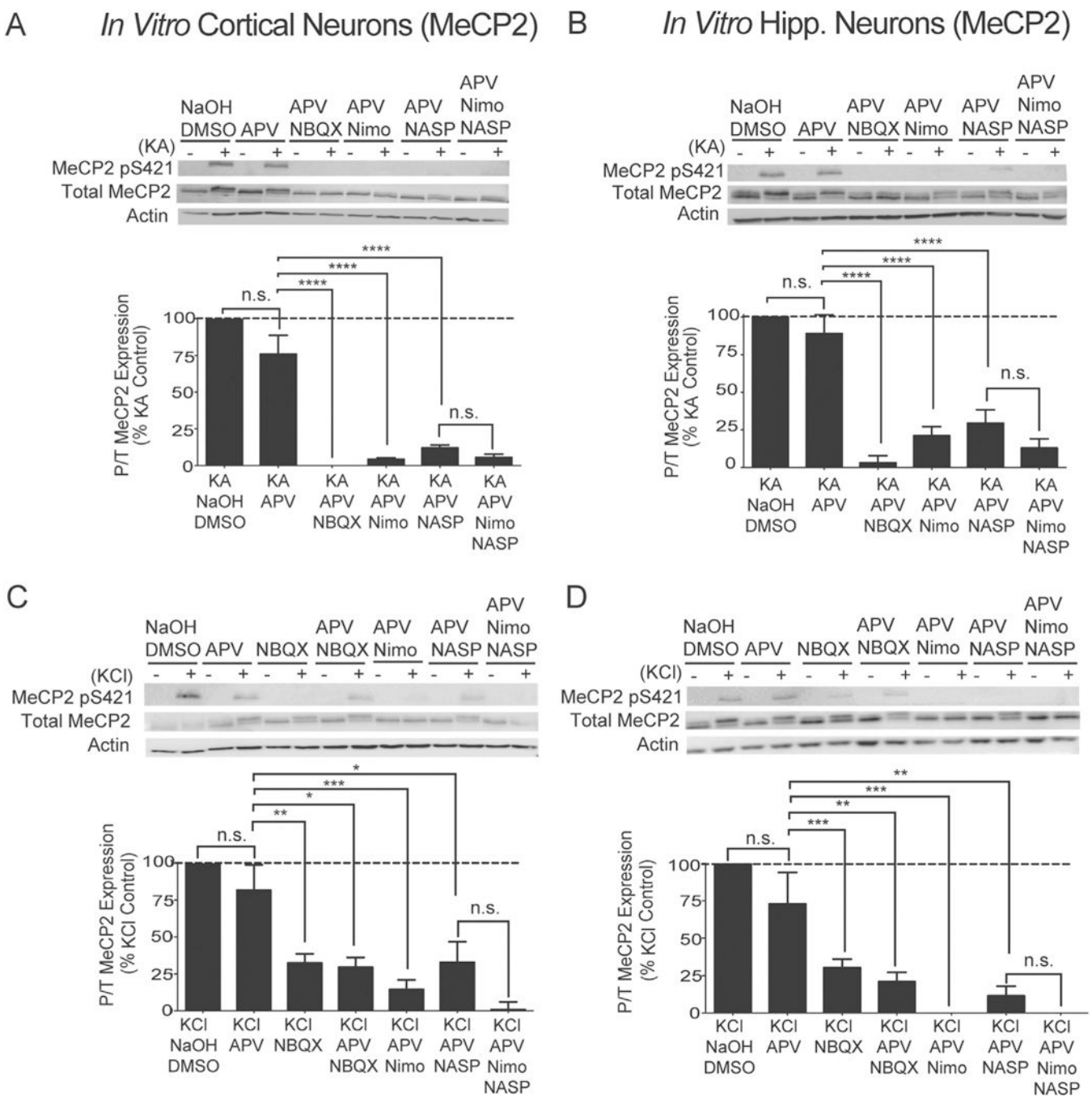

Fig. 3.

Kainic Acid (KA)- and KCl-induced MeCP2 S421 phosphorylation is mediated by CP-AMPARs and LT-VGCCs in E18 + 10DIV cortical and hippocampal neuronal cultures. Immunoblots demonstrating that KA still induced MeCP2 phosphorylation in the presence of D-APV in (A) C = cortical ($n = 4$, $p = 0.0722$) and (B) H = hippocampal ($n = 8$, $p = 0.8881$) cell cultures. However, MeCP2 phosphorylation was reduced from D-APV condition by adding NBQX (C: $n = 4$, $p < 0.0001$; H: $n = 8$, $p < 0.0001$), nimodipine (C: $n = 4$, $p < 0.0001$, H: $n = 7$, $p < 0.0001$), and/or NASPM (C: $n = 4$, $p < 0.0001$; H: $n = 6$, $p <$

0.0001). Addition of nimodipine to D-APV and NASPM did not further reduce MeCP2 S421 phosphorylation in cortical (p = 0.973) and hippocampal (p = 0.790) cultures. (C–D) Immunoblots demonstrating that KCl-induced phosphorylation of MeCP2 S421 cannot be reversed by treatment with D-APV alone in cortical (C: n = 4, p = 0.9637) and hippocampal (D: n = 4, p = 0.373) cultures. However, KCl-induced phosphorylation of MeCP2 S421 was reversed by NBQX alone in (C: n = 4, p=0.0069, H: n = 4, p = 0.0003). MeCP2 phosphorylation was reduced from the D-APV treated condition with the addition NBQX (C: n = 4, p = 0.0215; H: n = 4, p = 0.0082), nimodipine (C: n = 4, p = 0.0005; H: n = 4, p = 0.0002), and NASPM (C: n = 4, p = 0.0241; H: n = 4, p = 0.0015). Addition of nimodipine to D-APV and NASPM did not significantly further reduce p-MeCP2 S421 (C: p = 0.4352; H: p = 0.8012).

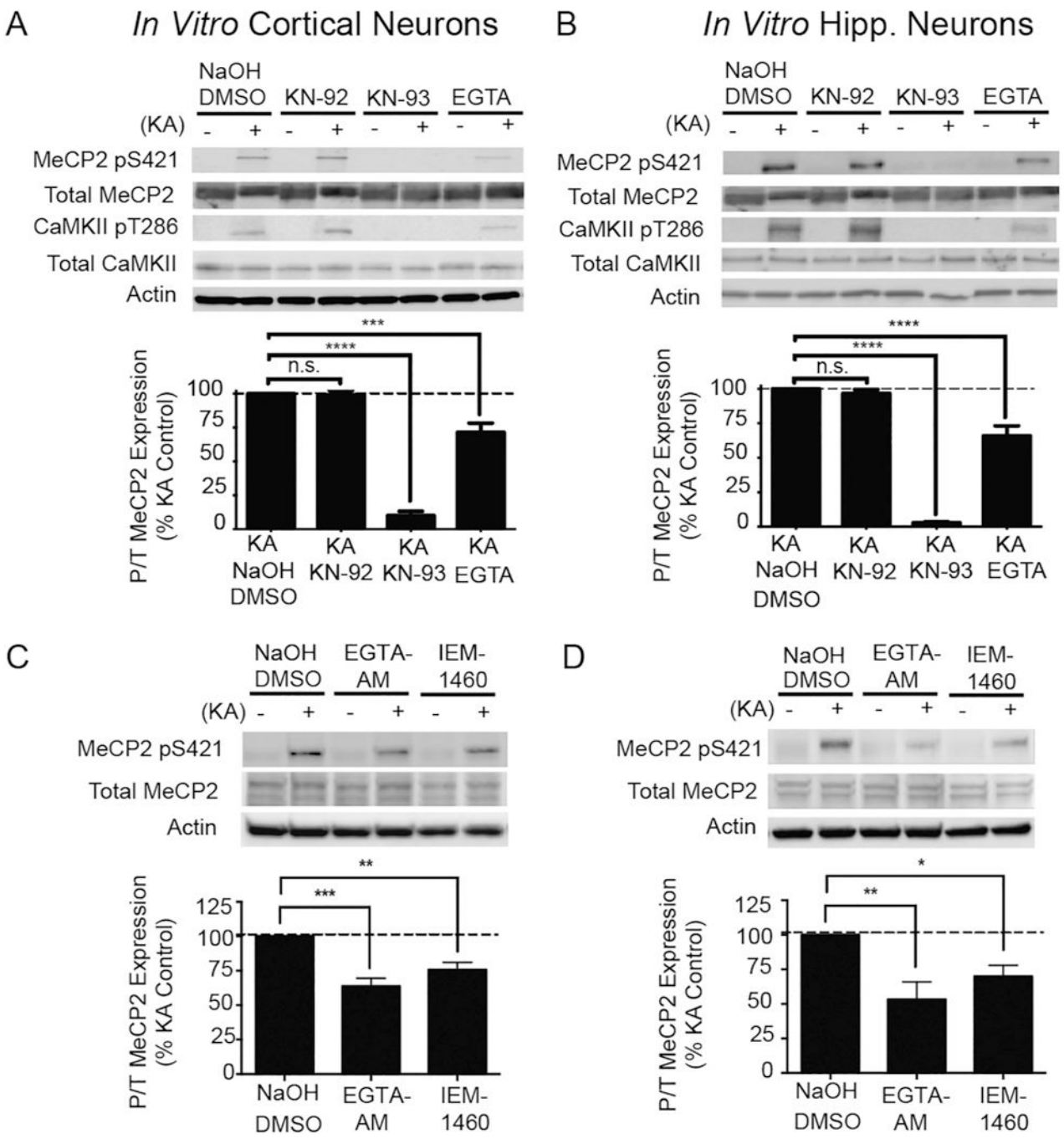

Fig. 4.

CaMKII T286 phosphorylation is upstream of MeCP2 S421 phosphorylation and mediated by intracellular Ca^{2+} in E18+10DIV neuronal cultures. (A–B) Representative immunoblots from cortical (A) and hippocampal cultures (B) demonstrating that KA-induced phosphorylation of MeCP2 S421 is reduced by treatment with the CaMKII inhibitor KN-93 (C: n = 5, $p < 0.0001$; H: n = 5, $p < 0.0001$), but not its inactive analog KN-92 (C: n = 5, $p > 0.9999$; H: n = 5, $p > 0.9999$). MeCP2 phosphorylation is reduced by the Ca^{2+} chelator EGTA (C: n = 5, $p = 0.0005$; H: n = 5, $p < 0.0001$). (C–D) MeCP2 Ser421 phosphorylation

is reduced by the membrane-permeable Ca^{2+} chelator EGTA-AM (100 μM) in cortical (C, 64 ± 6% *vs*. KA+Veh 100% condition, p = 0.0001) and hippocampal (D, 53 ± 13%, p = 0.0057) neuronal cultures. IEM-1460 (30 μM) reduces KA-induced MeCP2 phosphorylation in cortical (C, 76 ± 5%, p = 0.0039) and hippocampal (D, 70 ± 8%, p = 0.0361) cell cultures. n = 6 coverslips for cortical neurons and n = 4 for hippocampal neurons.

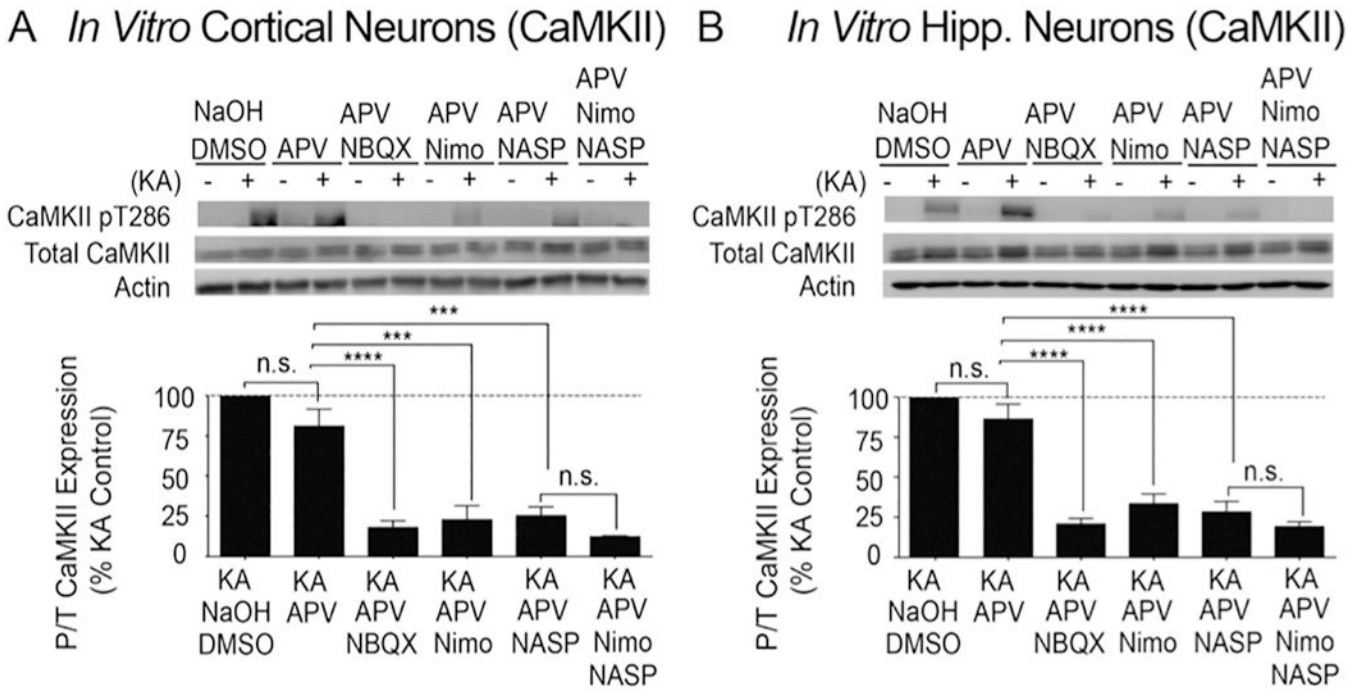

Fig. 5.

CaMKII T286 phosphorylation is partially mediated by CP-AMPARs and LT-VGCCs in E18+10DIV cell cultures. A–B, KA-induced phosphorylation of CaMKII T286 cannot be reversed by treatment with D-APV alone in cortical (A) ($n = 4$, $p = 0.2921$) and hippocampal neuronal cultures (B) ($n = 7$, $p = 0.5213$). However, CaMKII phosphorylation was reduced from the D-APV treated condition with the addition of NBQX (C: $n = 4$, $p < 0.0001$; H: $n = 7$, $p < 0.0001$), nimodipine (C: $n = 4$ $p = 0.0002$; H: $n = 6$, $p < 0.0001$), and NASPM (C: $n = 4$, $p = 0.0001$; H: $n = 6$, $p < 0.0001$). Addition of nimodipine to D-APV and NASPM did not further reduce CaMKII T286A phosphorylation in cortex ($p=0.7365$) or hippocampus ($p = 0.9290$).

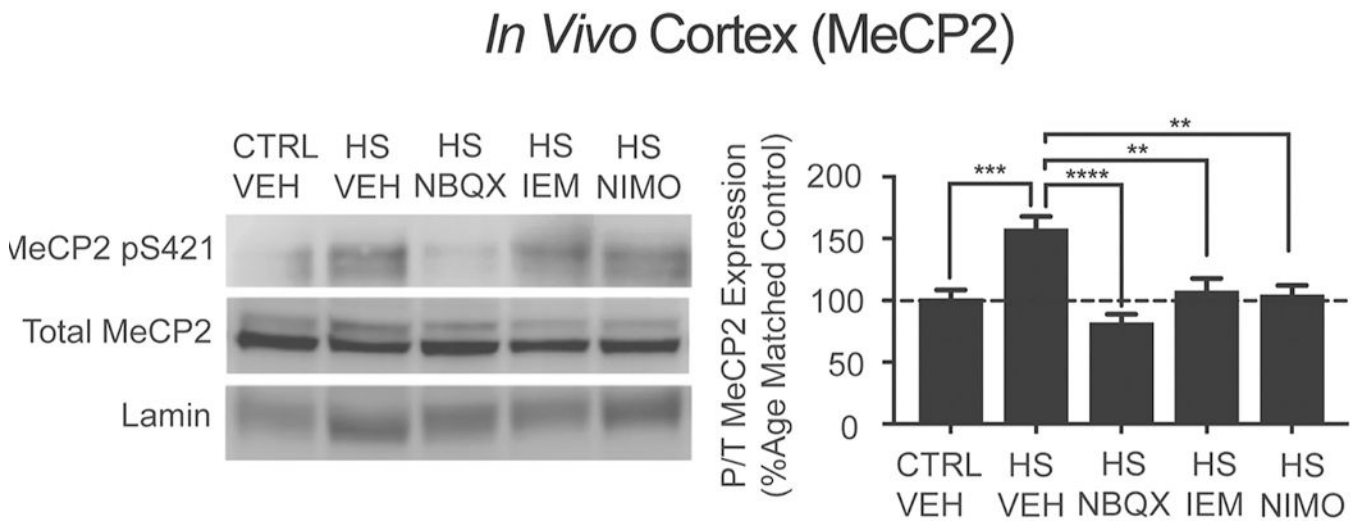

Fig. 6.

AMPARs and LT-VGCCs mediate hypoxic seizure (HS)-induced MeCP2 S421 phosphorylation in vivo in P10 rats. Increased MeCP2 S421 phosphorylation 3h. post-HS (HS+V: n = 17 *vs.* C+V n = 14, p = 0.0003) can be attenuated by in vivo pretreatment with the AMPAR antagonist NBQX (20 mg/kg, i.p.) (HS+NBQX: n = 9, *vs.* HS+V, p < 0.0001), the CP-AMPAR blocker IEM-1460 (20 mg/kg, i.p.) (HS+IEM-1460: n = 9, *vs.* HS+V p = 0.0099), or the LT-VGCC antagonist nimodipine (10 mg/kg, i.p.) (HS+NIMO: n = 9, *vs.* HS +V p = 0.0051).